Cable tray FIRE tests simulations in open atmosphere and in confined and mechanically ventilated compartments with the CALIF3S/ISIS CFD software

Sophie Bascou, Pascal Zavaleta, Fabrice Babik

Received: 9 March 2018 | Revised: 16 July 2018 | Accepted: 31 August 2018

DOI: 10.1002/fam.2680

SPECIAL ISSUE PAPER

WILEY

Cable tray FIRE tests simulations in open atmosphere and in confined and mechanically ventilated compartments with the CALIF3S/ISIS CFD software

Sophie Bascou | Pascal Zavaleta | Fabrice Babik

Institut de Radioprotection et de Sûreté Nucléaire (IRSN), Cadarache, St Paul-Lez-Durance Cedex 13115, France

Correspondence
Sophie Bascou, Institut de Radioprotection et de Sûreté Nucléaire (IRSN), Cadarache, St Paul-Lez-Durance Cedex 13115, France.
Email: sophie.bascou@irsn.fr

Summary

Fire hazard in nuclear power plants (NPPs) is particularly often investigated as potential cause of safety equipment failure and confinement loss. Many fire events recorded in NPPs involve electric cables, widely used throughout facilities. IRSN is developing the CALIF3S/ISIS computational fluid dynamics software devoted to fire simulation in large-scale confined and mechanically ventilated compartments. This paper presents two aspects of the CALIF3S/ISIS code ability to simulate fires. The first one concerns vertical and horizontal spreading of a cable tray fire in open atmosphere using an approach based on the FLASH-CAT cable fire spread model. Resorting to the suitable parameters of the FLASH-CAT model based on video fire analyses of tests enables to properly compute the heat release rate of the fire. The second aspect concerns the ability to simulate the evolution and consequences of fires in confined and mechanically ventilated compartments. For these cases, the heat release rate measured during the corresponding experiment is used as input data for the calculations. The predicted evolutions of pressure or gas temperatures are in relatively good accordance with the experiments. The major discrepancy concerns gas concentrations in the fire room which is attributed to a lack of information about the properties of the fuel material.

KEYWORDS

cable tray fire, computational fluid dynamics, ISIS, PRISME-2, tests

1 | INTRODUCTION

Fire hazard in nuclear power plants (NPPs) or nuclear reprocessing plants is particularly often investigated as it is a potential cause of safety equipment failure and confinement loss. Electric cables are a potentially large amount of fuel due to their plastic insulation material and to their wide use throughout the facilities.

Electric cable fire constitutes a twofold threat. In addition to the fire itself, cable fire is also associated to the loss of electric power and system control on the burning cable circuits. Electric cables can be involved in a fire in different ways: as the ignition source or as a fire spreading medium. More than 70 fire events from NPPs involving electrical cables as fuel were recorded in the current OECD FIRE Database between the late 1980s and the end of 2014.[1]

In this context, many efforts have been made in the last decades to prevent cable fires. Experimental programs have been carried out with the idea of increasing knowledge, offering risk mitigation ways and to promote the development and validation of predictive tools to evaluate the heat release rate of cable tray fires.

Sumitra performed cable trays fire in an open atmosphere in the 1980's to quantify the combustion behavior of cable trays.[2] Grayson conducted in the 2000's,[3] fire experiments involving cable trays in open atmosphere to provide an experimental database of reference cable fires for fire model validation. McGrattan carried out in the 2010's numerous cable tray fires in open atmosphere to propose empirical correlations for the heat release rate of such fires.[4,5]

In the framework of the OECD PRISME-2 program,[6] IRSN carried out a Cable Fire Spreading (CFS) campaign for investigating fire

spreading over complex fire sources and for evaluating fire consequences in confined and mechanically ventilated compartments. Two kinds of fire sources are studied: five horizontal cable trays arranged one above the others, and real open-door electrical cabinets with three overhead cable trays.[1,7] The five cable trays fire sources used in the CFS campaign were previously characterized in open atmosphere conditions during the CFS Support (CFSS) campaign.[8]

In addition to enhancing knowledge, the results of these experimental investigations also support the development and validation of the SYLVIA[9] fire zone code and the CALIF3S/ISIS[10] computational fluid dynamics (CFD) code, both developed by IRSN and used to support the fire Probabilistic Safety Assessment of French NPPs. The CALIF3S/ISIS software is based on the CFD approach by solving flow governing mass, momentum, and energy balance equations. The originality of the CALIF3S/ISIS software is its ability to take into account the interaction between the fire development and the ventilation network through the thermodynamic pressure. Modeling this interaction is essential for a detailed understanding of all the circumstances that can lead to a potential loss of containment.

In the early 2000's, an international benchmark exercise[11] listed as top issue the so qualified extremely complex determination of the heat release rate curve for cable tray fires. Considering this complexity and the developmental state of flame spread models, it was recommended to resort to heat release rates derived from tests conducted with a similar configuration, favoring the development of an experimental database. Predicting the heat release rate of cable tray fires is still qualified as highly complex in a more recent work.[12] Later on, among the PRISME 2 program, a benchmark exercise was performed, aimed at assessing the ability of fire modeling to predict a cable tray fire in confined and ventilated compartments. It was concluded that simulating cable fires in confined conditions is very complex by contrast with liquid fuel fire simulations that have a higher level of maturity. Predicting a cable tray fire has been challenging the fire community for years, and progress continues in an international research context.

This paper addresses the simulation of fire propagation on a cable tray stack in open atmosphere based on the CFSS-2 fire test from the CFSS campaign. The feature of this simulation is to use an empirical model for fire propagation together with prescribed vertical and horizontal spread rates from an experimental database. This is a step forward to predictive simulations of cable tray fires in open atmosphere provided that the macroscopic parameters of the fire source are known. Afterwards, two fire tests in confined and mechanically ventilated compartments are studied, namely CFS-3 and CFS-4 from the CFS campaign. The goal of the CFS test simulation is to evaluate the ability of the CALIF3S/ISIS software to predict the consequences of cable tray fires in confined and mechanically ventilated conditions. To do so, the simulations use the experimental values of the heat release rate as input data and are therefore called non-predictive. A comparison is then made with experimental values for quantities having a major importance in fire safety studies, ie, reflecting both the fire growth and the aeraulic behavior with its potential risk of loss of confinement. This is the mean whereby the accuracy of the CALIF3S/ISIS software predictions can be evaluated when the fire heat release rate is known. All these fire experiments use the same type of fire source (cable type and loading).

In order to present briefly the CALIF3S/ISIS software, the main characteristics of this code are discussed in Section 2. Then, Section 3 presents modeling and simulation results of the CFSS-2 fire test on the vertical and horizontal spreading of a cable tray fire in open atmosphere. It is based on the phenomenology of the FLASH-CAT model for cable fire spread[4] whose parameters have been determined through a video fire analysis process.[13] Section 4 presents modeling and simulation results of the two CFS-3 and CFS-4 fire tests concerning cable tray stack fires in confined and mechanically ventilated real scale compartments connected by an open door, for ventilation renewal rates (VRR) of 4 and 15 h^{-1}, respectively. To conclude, Section 4 gives a summary of the CALIF3S/ISIS capabilities and of some planned tasks in its development.

2 | DESCRIPTION OF THE CALIF3S/ISIS SOFTWARE

CALIF3S/ISIS is a simulation tool for fire development and assessment of fire consequences in confined and ventilated compartments (naturally and/or mechanically). It is a 3D field modeling code based on the CFD approach. CALIF3S/ISIS is an open-source software available at https://gforge.irsn.fr/gf/project/isis, with the associated documentation.

2.1 | Physical modeling

The CALIF3S/ISIS software can be used for incompressible or weakly compressible flows. During a fire, the highest plume velocities are roughly a few meters per second, and the flow is said to have a low Mach number. For low Mach number flows, a specific modeling is adapted to solve the time evolution of the thermodynamic pressure that is assumed to be uniform in space within the compartment (but potentially variable in time).

The modeled flow can be either laminar or turbulent. For the present paper, the turbulence modeling is achieved with the Reynolds and Favre averaged Navier-Stokes method, where the conservation equation of mass, momentum, and the conservation equation for the different scalars are written using the Favre average (density-weighted average) while density and pressure are averaged using the Reynolds formulation. Near the wall, where viscous effects are dominant, standard wall functions are used to take into account the boundary layers.

The combustion regime managed by the CALIF3S/ISIS software is non-premixed combustion. The turbulent combustion model[14] used for the present paper is the Eddy Dissipation Concept which is an extension of the Eddy Break-Up approach.[15] The combustion reaction is considered irreversible with an infinitely fast chemistry, and the mean chemical reaction rate is controlled solely by the turbulent mixture. Soot production is taken into account in the reaction through a constant coefficient, called soot conversion factor.

The general form of the energy equation for a multicomponent reacting system is extremely complex and is usually simplified for specific applications. For low velocity flows, such as fire induced flows, many widely used simplifications are possible. The viscous dissipation, the mixture kinetic energy, and the work due to buoyancy forces can

be ignored in comparison to the heat flux vector. As for turbulence modeling, near the wall, the convective flux is computed from wall functions using the laminar and turbulent Prandtl number. Finally, the conduction heat transfers in walls are modeled by a Fourier's equation. Due to the usually large geometrical dimensions of the fire surroundings, radiation significantly contributes to heat transfer and therefore to the flame development. Several radiative heat transfers modeling are available in the CALIF3S/ISIS software such as the spherical harmonic approximation P-1 or the finite volume method. The finite volume method[16,17] is selected for the present study. The impact of soot on radiation is taken into account through the absorption coefficient, which is defined by the sum of gas and soot absorption coefficients. To define the absorption coefficient, the weighted-sum-of-gray-gases model[18] is selected for this study and the soot absorption coefficient is computed from a correlation depending on temperature and the soot volume fraction.

2.2 | Numerical properties

The equation system solved by the CALIF3S/ISIS software comprises eight tightly coupled balance equations: the mass balances (global, fuel, and mixture fraction), the momentum and energy balances, the transport equations for turbulent energy k and its dissipation rate ε and, finally, the radiation intensity balance equation describing radiative heat transfer.

The discretization in time and space is made using a finite volume method to obtain schemes that achieve a good compromise between time cost and accuracy and ensure that unknowns stay within their physical boundaries. Second-order upwinding techniques are used to accurately take into account fast spatial variations in unknowns (eg, at the flame front or close to walls), without stability loss.

To make CALIF3S/ISIS more efficient and robust, temporal discretization is carried out with a fractional step scheme,[19] ie, the equations are solved in sequence. Finally, CALIF3S/ISIS is based on the PELICANS scientific computing development platform (IRSN open-source software, http://gforge.irsn.fr/gf/project/pelicans).

Many results have already been obtained with the CALIF3S/ISIS software with respect to a substantial validation matrix.[20] In the present document, separate effect tests are investigated focusing on fire propagation modeling in open conditions (Section 3) and fire simulation in confined conditions with two VRRs (Section 4).

3 | SIMULATION OF THE CFSS-2 FIRE TEST (CABLE TRAY FIRE IN OPEN ATMOSPHERE)

3.1 | Description of the fire experiments

The CFSS tests are carried out on a set of five horizontal cable trays arranged one above the other. This campaign allowed characterizing fire sources in open atmosphere conditions under the large-scale calorimeter of the IRSN SATURNE facility, described below.

The fire source consists of five horizontal cable trays vertically arranged one above the other (Figure 1). Every cable tray is 3.0 m long, 0.45 m wide, and 0.05 m high. There is a constant vertical spacing of 0.3 m between trays. Cable samples are 2.4 m long and are loosely packed.

FIGURE 1 Set of cable trays used for the CFSS fire tests [Colour figure can be viewed at wileyonlinelibrary.com]

The CFSS-2 test involves a cable-type used as control cable in NPPs. This cable-type contains poly (ethylene/vinyl acetate) (EVA) and polyethylene (PE) as polymeric materials and aluminum tri-hydrate (ATH) as halogen free flame retardant (HFFR).[21] Its diameter is 20.0 mm, and its mass per unit length is about 570 kg/km. Every tray is filled with 32 cable samples.

The ignition of cable trays is triggered by a propane sand burner. The burner is 0.3 m by 0.3 m, and its top face is located 0.2 m below the bottom of the first tray almost halfway along. The burner supplies a fire power of 80 kW during 12 minutes 24 seconds. The starting time of the burner operation corresponds to the onset of the test. The five cable trays are set-up against an insulating wall and their

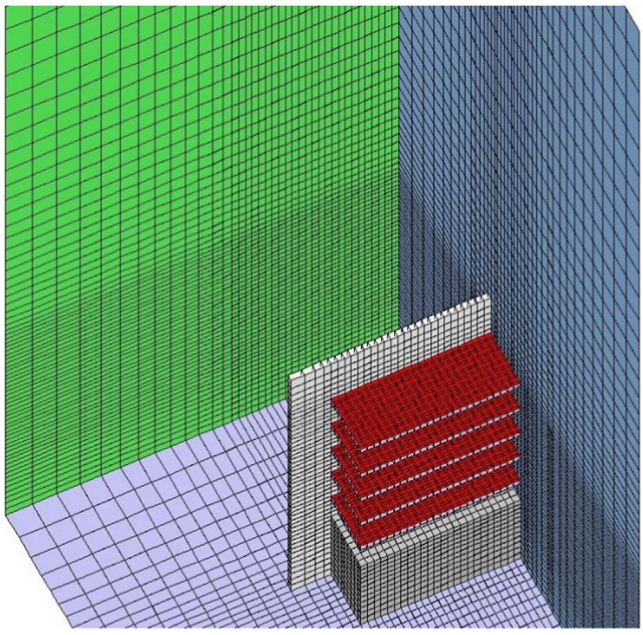

FIGURE 2 View of the fire source modeling with the CALIF3S/ISIS software [Colour figure can be viewed at wileyonlinelibrary.com]

weights are continuously measured by a weighting system located just beneath.

3.2 | Modeling of the fire test

The CALIF3S/ISIS modeling of the fire test is made similar to the experimental setup, ie, the five horizontal cable trays are individually modeled (see Figure 2). The aim is to model fire propagation, whether it is along a single tray or from one tray to another.

3.2.1 | Facility modeling and BC description

The CFSS-2 test is performed under a large-scale calorimeter located in a very large facility, ie, under open atmosphere condition. This facility, called SATURNE, is 20 m high and its volume is about 2000 m^3. The fluid domain is modeled large enough around the fire source to avoid any disturbance. The entire fluid domain is parallelepipedic such that it is 5.9 m long, 3.65 m wide, and 6.0 m high. For comparison purposes, the cable tray stack is 2.4 m long, 0.45 m wide, and 2.19 m high (from the ground). A symmetry condition is used in a vertical plane (blue wall on the right on Figure 2) halfway along the cable trays in order to reduce the size of the modeled domain. Finally, it becomes 2.95 m long (instead of 5.9 m) with 1.2-m-long trays. This symmetry condition in the modeling of the fire spread is allowed by the symmetric behavior of the fire spread observed in the experiment. The boundary condition on the three other vertical borders and the upper border of the fluid domain is "inlet-outlet" so that flow can enter and leave the domain.[14] The floor is modeled as a concrete wall (0.35 m thick), and conduction through it is taken into account.

Concerning the fire source, cable trays are solid slabs 0.45 m wide and 0.05 m high with constant 0.3-m spacing between trays. The "fire" boundary condition is modeled by means of an "inflow" boundary condition[14] that enables to model a fuel mass flowrate entering the domain. It is applied on the top faces of the cable trays, the remaining ones being adiabatic. The fire boundary condition is detailed in Section 3.2.3.

Due to its obstruction, the weighting system located beneath the tray stack is removed from the fluid domain. It has a simplified rectangular shape with the same length and width as cable trays. It is 0.74 m high, and it is 0.20 m away from the first cable tray. The insulated support wall at the back of the cable trays is also removed from the fluid domain. The boundary condition on these parts is set as adiabatic.

3.2.2 | Meshing and time step

The fluid domain meshing features mesh varying in size depending whether they are close to the outer edges of the modeling or close to the fire source (see Figure 2). The total mesh number for the fluid domain is about 104 000. The mesh size range is presented in Table 1.

The time step used for the calculation is 0.05 seconds over the 3500 seconds of the scenario.

3.2.3 | Fire source modeling

This section presents the CALIF3S/ISIS modeling of the combustion of the HFFR cables used for this test and of the fire propagation based on a FLASH-CAT-like phenomenology.

TABLE 1 Mesh sizes for CFSS-2

	Fire Room
x-axis	5 cm to 20 cm
y-axis	5 cm to 20 cm
z-axis	5 cm to 40 cm

Chemical reaction

In order to determine the appropriate equation to represent the combustion reaction of the HFFR cables, the composition of these cables has to be looked closer. The main materials, reacting to thermal stress, identified by chemical analyses, are the PE and the poly (ethylene/EVA) copolymer (PE/EVA) and ATH. The mass fraction of these components has been determined as follows: 40% PE/EVA, 60% ATH.[21]

The chemical formula of the poly (ethylene/EVA) copolymer is $(C_2H_4)_n$-$(C_4H_6O_2)_m$. Unfortunately, the chemical analyses are not able to give the ratio (basically, to determine "n" and "m") between PE and EVA. It is underlined that the contribution of PE instead of EVA would lead to higher oxygen consumption and higher carbon dioxide production. Indeed, PE (chemical formula C_2H_4) does not contain any oxygen, and its molar mass (M_{PE} = 28 g/mol) is about three times lower than the EVA ($C_4H_6O_2$, 86 g/mol) one. The extent of these modifications depends on the mass composition of PE and EVA. For the simulation needs, it is supposed that coefficients "n" and "m" are equal, and that "n" accounts for the PE from the single polymer and the PE from the PE/EVA copolymer, so that the considered material for PE-PE/EVA is $C_6H_{10}O_2$.

The characteristics of the two different components are listed below:

- PE/EVA:

Its chemical formula is $C_6H_{10}O_2$, its molar mass is $M_{PE/EVA}$ = 114 g/mol, this "equivalent" copolymer is reactive to fire, it produced combustible pyrolysis gas. Its combustion reaction is as follow:

$$C_6H_{10}O_2 + (7.5\text{–}0.5\ co\text{–}s)\ O_2 \rightarrow (6.0\text{–}co\text{–}s)\ CO_2 + 5\ H_2O + co\ CO + s\ C$$

Obviously, this component has to be taken into account in the combustion reaction given as inlet data for the CALIF3S/ISIS calculation.

- Alumina tri-hydrate:

Its chemical formula is $Al(OH)_3$, its molar mass is M_{ATH} = 78 g/mol, this flame retardant reacts under thermal stress due to the fire, ie, it partially pyrolyses thus generating incombustible products, the remaining mass being inert mineral residue (alumina):

$$2\ Al(OH)_3 \rightarrow Al_2O_3 + 3\ H_2O$$

Considering the different molar masses of the products, then it comes to:

$$1000\ g\ ATH \rightarrow 654\ g\ alumina + 346\ g\ water$$

Therefore, 1 kg of ATH gives about 65% inert solid alumina and 35% water vapor. Alumina is a solid residue that is not taken into account in the experimental mass loss measure as it remains on the cable trays. For this reason, it is not considered. However, the water vapor production has an impact on the local atmosphere of the fire room and then must be considered.

Tables 2 and 3 summarize the different mass fractions of products as a percentage of the total mass of cable and as a percentage of the total mass of gas released.

Regarding chemistry, the combustion of PE/EVA contained in cables produces carbon dioxide, carbon monoxide, water vapor, and soot. In addition, ATH produces water vapor. Since, in the CALIF3S/ISIS CFD software, only one fuel can be implemented, it becomes necessary to resort to an equivalent fuel to represent both PE/EVA and water from ATH. At this point, it must be reminded that the mass loss rate (MLR) measured in the experiment corresponds to the PE/EVA pyrolysis gas release and to the water vapor release by ATH (minor cable components are neglected).

From Table 3, it can be observed the composition of the pyrolysis gas that must be taken into account. Considering the molar masses of $C_6H_{10}O_2$ and H_2O and the mass composition presented in Table 3, the equivalent fuel should combine about 0.6 mole of $C_6H_{10}O_2$ per 1.8 mole of H_2O which gives $C_{3,6}H_{9,6}O_3$ and the following equivalent one-step irreversible combustion with infinitely fast chemistry reaction:

$$C_{3,6}H_{9,6}O_3 + (4.5\text{–}0.5\ co\text{–}s)\ O_2 \rightarrow (3.6\text{–}co\text{–}s)\ CO_2 + 4.8\ H_2O + co\ CO + s\ C$$

where *co* and *s* represent the stoichiometric coefficients of carbon monoxide CO and soot C, respectively.

The carbon monoxide and soot yields* measured in the experiment are 0.027 and 0.015 (g/g) for the CFSS-2 fire test.[8] Therefore, the stoichiometric coefficients co for carbon monoxide and s for soot are defined as follows in the CALIF3S/ISIS modeling:

$$co = \frac{M_{C_{3,6}H_{9,6}O_3} \times y_{co}}{M_{CO}}$$
$$s = \frac{M_{C_{3,6}H_{9,6}O_3} \times y_{soot}}{M_C}$$

where:

- $M_{C_{3,6}H_{9,6}O_3} = 100.8$ g/mol, is the molar mass of the equivalent combustible fuel $C_{3,6}H_{9,6}O_3$,
- M_C = 12.0 g/mol, is the molar mass of carbon C,
- M_{CO} = 28.0 g/mol, is the molar mass of carbon monoxide CO,
- y_{soot}, is the soot yield given by the experiment,
- y_{co}, is the carbon monoxide yield given by the experiment.

The energy release of this combustion reaction is set at the experimental value of the average effective heat of combustion (EHC) = 27 MJ/kg.

*Despite the fact that soot is a minor combustion product, it has to be taken into account regarding radiative heat transfer calculation by the ISIS software.

TABLE 2 Cable product mass composition

PE/EVA	Alumina	Water	Total
40%	40%	20%	100% cable mass

TABLE 3 Pyrolysis gas mass composition

PE/EVA	Water	Total
67%	33%	100% mass of released gas

It must be highlighted that the proposed equation reaction with $C_{3,6}H_{9,6}O_3$ is suggested in order to take into account the amount of water vapor released by ATH and measured by the weighting system. However, it is not representative of what happens in the experiment in so far as this equation is an average over the total duration of the test. Indeed, alumina trihydrate releases water vapor when cable temperatures are between 80°C and 205°C according to Brossas[22] or between 180°C and 400°C in the more recent reference.[23] A second difficulty can be underlined concerning the first period of the transient. It deals with the propane burner operation. Using HFFR cables requires a long burner operation which is not negligible (12 minutes 24 seconds). Moreover, the 80 kW supplied by the propane burner (the propane effective heat of combustion is about 46 MJ/kg, and its molar mass is 44 g/mol) represents a significant contribution to the recorded heat release rate (HRR) on that period. Therefore, in the CALIF3S/ISIS modeling, $C_{3,6}H_{9,6}O_3$ combustion is substituted to propane combustion, thus leading to possible discrepancies from the experiment in terms of chemistry.

Fire propagation on the cable trays

The approach is to model fire propagation along trays and from one tray to another based on the tray stack modeling (see Figure 2) and the FLASH-CAT phenomenology.[4]

The FLASH-CAT model (FLAme Spread over Horizontal CAble Trays) is aimed at predicting the HRR of a fire spreading within a vertical stack of horizontal cable trays. Hypotheses used by the FLASH-CAT model suggest that the fire should propagate upward through the cable trays depending on an empirical timing sequence only based on the tray order in the stack and assumes that, once ignited, the cables burn over a length that is greater than that of the tray below (see Figure 3). The burning pattern has therefore an expanding V-shape as there is an increasing length of cable that initially ignites when fire propagates upwards and due to lateral propagation of fire. As the mass of combustible material at the center of the V is consumed, a horizontal extinction front may appear at the center of the trays and the V-shape may become an open wedge until the full length of cable is burnt. For information purposes, this observation was made on the CHRISTIFIRE experiments[4] used to elaborate the FLASH-CAT model; however, it is not the case in the CFSS campaign.

It is highly underlined that some model parameters from McGrattan et al[4] were deduced from observations made on only one fire test involving 14 horizontal cable trays divided in two arrays of seven horizontal trays.[24] Those parameters have been re-evaluated for the CFSS tests through video fire analyses.[13] The model and parameters used are presented below for the CFSS-2 test (values at ignition are denoted by "P_0" where "P" is the parameter of interest):

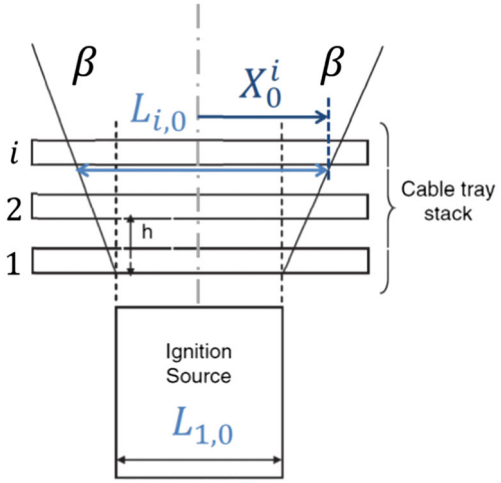

FIGURE 3 Model for fire propagation in a cable tray stack (based on the work of McGrattan et al[4]) [Colour figure can be viewed at wileyonlinelibrary.com]

- The burning length at tray ignition: $L_{i+1,0} = L_{i,0} + 2h_{tray} \times \tan(\beta)$
  - With
    - i, the tray number in the stack
    - h_{tray}, the tray spacing (0.30 m)
    - β, the angle (as shown on Figure 3) evaluated at 9.07°
    - $L_{1,0}$, the burning length of the first tray, it equals the burner length (as shown on Figure 3, ie, 0.30 m)
- The horizontal spread rate S_i: 0.81, 1.07, 2.73, 2.97, and 6.41 mm/s for tray #1 to #5
- The vertical spread rate defined as tray ignition times $t_{ign,i,0}$: 263.5, 396.0, 603.0, 741.0, and 834.0 seconds for tray #1 to #5
- The constant fire duration Δt: 1500 seconds
- The combustible mass per unit area of cable tray m_C'': 17.96 kg/m^2, calculated as the ratio of the total mass loss (TML = 97 kg ± 7) during CFSS-2 and the total surface of the five trays (S_{tot} = 5.4 m^2)
- The heat of combustion $\Delta H_{c,eff}$: 27 MJ/kg, it is the effective heat of combustion measured during the experiment
- The equivalent† average HRR per unit area of cable tray in the proposed modeling $\dot{q}_{avg}''$: 388 kW/m^2, calculated using $\Delta t = \frac{m_C'' \Delta H_{c,eff}}{5 \times \dot{q}_{avg}''/6}$.[4]

The implementation of the fire propagation modeling in the CALIF3S/ISIS software is based on the calculation of the ignition time $t^i(x)$ (at the distance x from the center of cable tray i) and the calculation of the burning rate $\dot{m}_i''(x,t)$.

†This value of the average heat release rate per unit area is an equivalent value used for modeling. It is expressed per unit area of cable tray as it is modeled, ie, by a 2D surface in the ISIS software. It should not be confused with the average heat release rate per unit area of the cable surface (as a 3D element) and measured under cone calorimeter. The relationship between the two values of the average heat release rate per unit area can be evaluated through geometric considerations and is about: $\dot{q}_{avg}'' \approx 4.468 \dot{q}_{avg,bs}''$. For information purposes, the bench scale value for the considered cables is about $\dot{q}_{avg,bs}'' \approx 90 kW/m^2$.

It is emphasized that the implementation in the CALIF3S/ISIS software allows asymmetric fire propagations between the right-hand side and the left-hand side of a tray. For that reason, let X_0^i represent the burning length at tray ignition in one direction of the tray, measured from the center of the tray (see Figure 3). In case of a symmetric fire propagation, then $L_{i,0} = 2 \times X_0^i$.

The ignition time at the x abscissa of cable tray i is given as follows:

- if $x < X_0^i$, therefore, x belongs to the burning length at tray ignition and its ignition time is $t_{ign,i,0}$ model parameter given as inlet data,
- if $x > X_0^i$, the time at which the fire reaches the x abscissa depends on the horizontal spread rate as follows:

$$t^i(x) = t_{ign,i,0}^i + \frac{x - X_0^i}{S_i}$$

The burning rate calculation takes into account the ignition time as well as the fire development according to Figure 4. The evolution of the mass-rate $\dot{m}_i''(x,t)$ presented in Figure 4 is taken from the evolution of the HRR given in McGrattan et al[4] with the following ratio:

$$\dot{m}_{avg}'' = \frac{\dot{q}_{avg}''}{\Delta H} \text{ in } kg.s^{-1}m^{-2}.$$

The fire duration is recalculated by the CALIF3S/ISIS software by integrating the mass-rate profile given in Figure 4, in order to ensure that the burning mass does not exceed the available fuel mass per unit area:

$$\int_{t^i(x)}^{\Delta t + t^i(x)} \dot{m}''(t)dt = m_C''.$$

To summarize, through this phenomenology, the CALIF3S/ISIS software is able to calculate for every mesh the boundary condition on the fire surface (see red area in Figure 2), ie, the time evolution of the MLR from ignition to fire extinction.

3.2.4 | Turbulence modeling

Turbulence is modeled by means of the standard $k - \varepsilon$ model. The model parameters used are the constant default values of the CALIF3S/ISIS

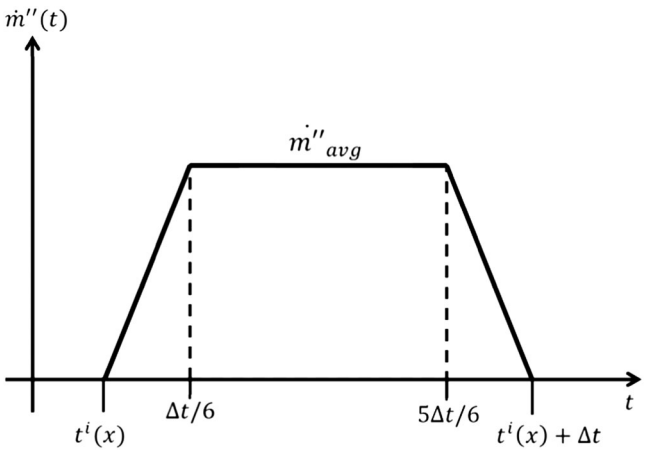

FIGURE 4 Outline of the mass-rate per unit area

CFD software.[14] The turbulent production due to buoyancy effects is modeled with the Generalized Gradient Diffusion Hypothesis.

3.2.5 | Radiative heat transfer modeling

The radiative heat transfer modeling used in this study is the finite volume method.[14] The discretization of the angular space is automatically set by the software, and the number N of discretization per octant used is the advised value $N = 4$ (default value).

3.3 | Simulation results

Figure 5 shows the evolutions of the MLR and of the HRR for the experiment and for the simulation.

Concerning the experimental results, a delay can be observed between the MLR rise and the HRR rise. This is due to the water release by the fire retardant ATH. Indeed, when cables are heated (see Section 3.2.3.1), ATH contained in the cables undergoes decomposition into water vapor and solid alumina. Alumina remains on the cable trays, but water vapor is released. Consequently, its corresponding mass loss is recorded by the weighting system located below the cable tray stack. This water mass loss is associated with no heat release, which explains the observed delay.

The comparison between the experimental results and the simulated ones indicates that this delay between the MLR and the HRR is not predicted as curves start rising at the same time. This is due to the fact that only one fuel is considered in the CALIF3S/ISIS modeling as ATH is taken into account by resorting to an equivalent fuel (see Section 3.2.3.1). It must be highlighted that the video fire analysis method[13] used to determine the optimized parameters for the FLASH-CAT model (see Section 3.2.3.2) is based on the observation of flame fronts. As a consequence, the spread parameters are representative of the combustion process by opposition to the degradation process of ATH that releases vapor. For that reason, it is not possible to predict the earlier MLR due to ATH. Nevertheless, it can be observed that the MLR rise is predicted properly with a suitable slope despite this slight delay. The MLR peak is quite well predicted (76 g/s for the simulation against 78.5 g/s for the experiment which represents an about 3% discrepancy). The HRR increase is very well predicted by the CALIF3S/ISIS software. Concerning the HRR peak, it is also well predicted. About the downward trends of the MLR and HRR curves, it can be noticed that the decrease is underestimated during the first 500 seconds, and then it is predicted too sharp and the end of the fire scenario is predicted too early. Actually, the fire end in the experiment is representative of a slow decay phase of the fire which may not be properly reproduced through constant horizontal spread velocities and by the considered mass-rate evolution shown in Figure 4. The TML and the total heat release predicted by the CALIF3S/ISIS software are, respectively, 97 kg and 2657 MJ; this is to be compared with the experimental values of 97 kg and 2550 MJ. The total heat release is slightly overestimated by about 4%, which remains close to the experimental value. On a safety point of view, the major discrepancy on the predicted fire behavior is observed on the decay phase so that the simulation result is conservative on this part of the transient as it favors a longer period at high fire power. In fact, the right amount of energy and the right amount of mass loss are predicted by the CALIF3S/ISIS software but on a shorter period of time.

Figure 6 gives illustrations of the temperature fields predicted by the CALIF3S/ISIS software at several times thus allowing a visualization of flame front spread from one tray to another as well as the horizontal propagation as described in the FLASH-CAT approach. It is considered that the temperature of a flame is 600°C (873 K)[25]; these flames are colored from green to red in Figure 6. The three upper pictures at $t = 800$, 1200, and 1600 seconds show the fire growth as the burning surface is increasing due to both the upward and sideward spread up to when all the cable trays are on fire all over their length at about $t = 1600$ seconds. This time corresponds to the MLR and HRR peaks predicted by the CALIF3S/ISIS software. Afterwards, on the three lower pictures at $t = 1800$, 2200, and 2600 seconds, the extinction front appears on the lowest tray and it propagates upward and sideward, similarly to the

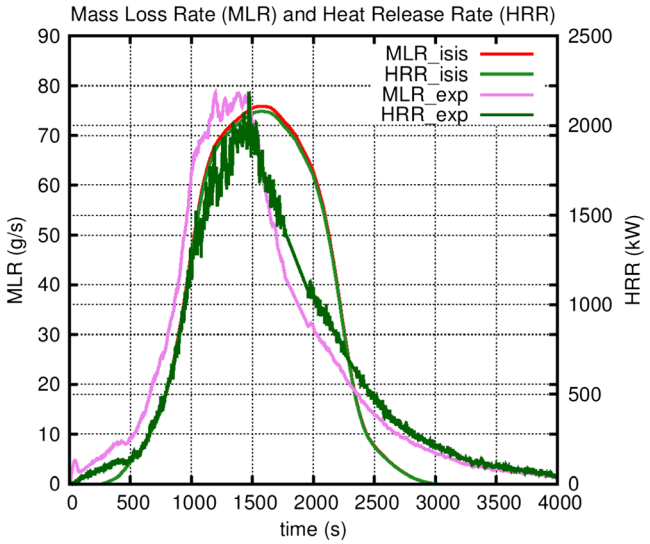

FIGURE 5 Mass loss rate and heat release rate for the CFSS-2 fire test, experiment, and simulation [Colour figure can be viewed at wileyonlinelibrary.com]

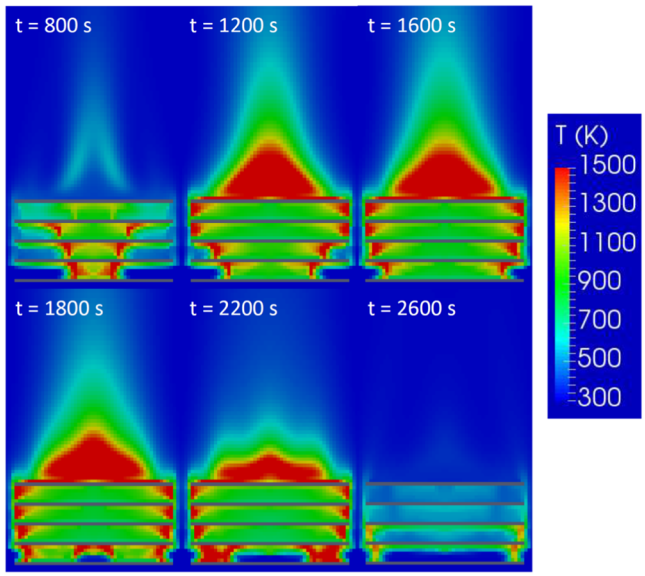

FIGURE 6 Visualizations of fire spread simulated with CALIF3S/ISIS at several times [Colour figure can be viewed at wileyonlinelibrary.com]

ignition front. The MLR and HRR decrease as the extinction front goes on until fire is totally extinguished.

4 | SIMULATION OF THE CFS-3 AND CFS-4 FIRE TESTS IN CONFINED/VENTILATED ROOMS

4.1 | Description of the fire experiments

The CFSS campaign presented in Section 3.1 was a preliminary step for the CFS campaign, performed in confined and mechanically ventilated conditions in the multi-room DIVA facility.[1] The fire sources used in the CFS campaign are the same as those characterized during the CFSS campaign (see Figure 1).

As illustrated in Figure 7, the DIVA facility features:

- three rooms (about 6 m in length, 5 m in width, 4 m in height),
- a common corridor (15.6 m in length, 2.5 m in width, 4 m in height),
- and a fourth room (8.8 m in length, 5 m in width, 4 m in height) located above both room 3 and the corridor.

Walls are 0.3 m thick and are made of reinforced concrete. The vertical walls of the fire room are covered by a 0.05-m layer made of concrete to prevent any damage on the bearing walls. The reinforced concrete and the sacrificial concrete are separated by a 1.5-cm-thick air slot. The ceilings of the fire room and adjacent room are covered by a 0.06-m and 0.03-m-thick layer of insulation (Thermipan), respectively.

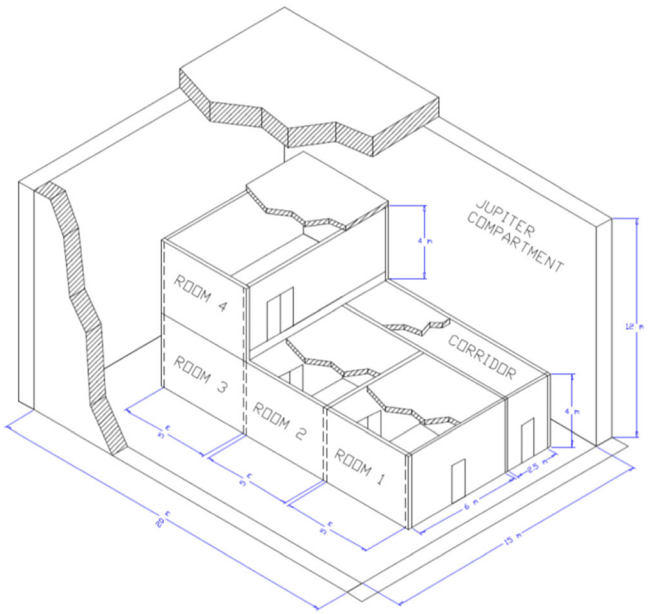

FIGURE 7 Bird's eye view of the DIVA facility inside the JUPITER compartment [Colour figure can be viewed at wileyonlinelibrary.com]

The DIVA facility is also equipped with a ventilation network including both air supply and exhaust circuits.

For CFS-3 and CFS-4 tests (see Table 4), only two rooms of the DIVA facility are involved, namely room R1 and room R2. Room R1 (the fire room) and room R2 (the adjacent room) are connected by an open doorway (0.79 m × 2.17 m). In this configuration, the ventilation system is composed of one inlet duct in the fire room and one exhaust duct in the adjacent room. Both inlet and exhaust ducts are 0.45 m × 0.3 m × 0.7 m with a blowing surface area 0.3 m in width and 0.6 m in height. Front and top view schemes of the facility and experimental device are presented in Figures 8 and 9 for more details.

Table 4 gives the operating conditions of the cable tray CFS tests in terms of duration of the propane burner ignition and of VRRs provided by the ventilation network. The test from the CFSS campaign carried out in open atmosphere is also mentioned in this table. The VRR is defined as the number of room volume renewed per hour. For example, as rooms R1 and R2 have a total volume of about 240 m^3, then the flowrate is expected to be initially about 960 and 3600 m^3/h for VRR of 4 and 15 h^{-1}, respectively.

4.2 | Lessons learnt from the experiment

The main outcomes of the CFS campaign presented in this section are taken from document.[1] For a more comprehensive view of the experimental results and analysis, reference should be made to the abovementioned document.

It is reminded that the CFS fire tests were performed on two kinds of cables: HFFR cables for CFS-3 and CFS-4 tests and halogenated flame-retardant cables for the other CFS tests. Two VRRs were investigated: 4 h^{-1} for CFS-3 and 15 h^{-1} for CFS-4. The fire sources used in the CFS campaign were previously characterized under a large-scale calorimeter in open atmosphere during the CFSS campaign.

The first outcome concerns the amount of fuel burnt during the CFS tests compared with that of the CFSS tests. It is concluded that the TML for CFS tests with high VRR is identical to the one for the CFSS tests, while the TML is lower for CFS tests with low VRR. Every CFS test fire burns for a longer time than in open atmosphere and is characterized by lower peaks of MLR and HRR. When the VRR is at its lowest value, the CFS tests show reduced combustion efficiencies. Conversely, with the highest value of the VRR, combustion efficiency is observed as similar to that in open atmosphere for CFS-4. The CFS-3 fire test, classified as under-ventilated, shows an increase in the production of unburnt hydrocarbons accumulating under the ceiling of the fire room. These accumulations of unburnt hydrocarbon gases lead to eight consecutive combustions in the upper part of the fire room associated with HRR peaks of 0.5 MW for CFS-3 (see Figure 11). It is underlined that a major fire

TABLE 4 Matrix of the cable tray fires for CFS tests

Test	Cable Type	Burner Operation	VRR, h^{-1}	Test in Open Atmosphere
CFS-3 CFS-4	Halogen free flame retardant (HFFR) control cable	12 min 24 s	4 15	CFSS-2

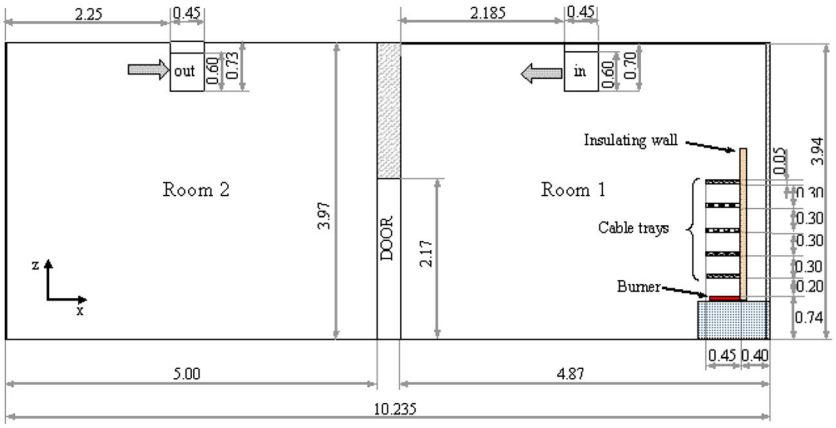

FIGURE 8 Front view of the experimental facility (R1 and R2) [Colour figure can be viewed at wileyonlinelibrary.com]

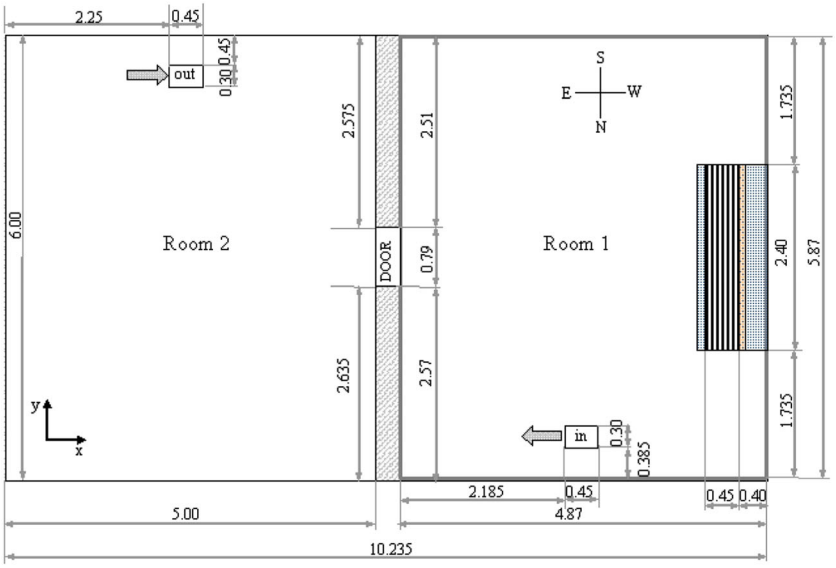

FIGURE 9 Top view of the experimental facility (R1 and R2) [Colour figure can be viewed at wileyonlinelibrary.com]

consequence is attributed to those repetitive combustions leading to the highest peaks of gas temperature and heat flux (near the ceiling) as well as pressure rises.

4.3 | CALIF3S/ISIS modeling

Both the fire room and the adjacent room are modeled as well as the doorway (see Figure 10) by means of a composed meshing allowing several concatenated meshing in the CALIF3S/ISIS CFD software. A particular attention has to be paid to the conformity of the different meshing.

4.3.1 | Facility modeling and boundary conditions description

Concerning the outer structural walls, conduction within the walls is calculated (see Section 4.3.2 for material properties), and the heat exchange condition with the outside is set as adiabatic. For the calculation of the convective heat transfer coefficient, wall functions are used and the laminar and turbulent Prandtl numbers are set at the same value of 0.7 (see CALIF3S/ISIS software[14]). This is also the case for ceilings, but material properties are implemented accordingly (see Section 4.3.2). The separation wall between the fire room and the adjacent room differs from the other walls in that the conductive heat transfer is calculated within the wall and heat exchange conditions at the middle of the wall is an imposed temperature equal to the initial wall temperature at the beginning of the fire scenario.

In-room inlet and outlet openings of the aeraulic circuits are modeled by removing the corresponding cells from the fluid domain. The appropriate boundary condition on these holes is "pipe-junction" (see CALIF3S/ISIS software,[14] for more details). It makes it possible to control the flow directions, flowrates, and aeraulic resistances of the ventilation system. The general Bernoulli equation is solved at each branch and enables to take into account pressure variations over time in the confined and mechanically ventilated compartment.

As for the simulation of the CFSS-2 fire test, the weighting system and the fluid slice between the West wall and the insulated support wall at the back of the fire source are removed from the fluid domain and the boundary condition is set as adiabatic.

The fire source is made similar to the experimental setup as explained in Section 3.2.1, ie, trays are individually modeled. Fire propagation is simulated by prescribing the mass flowrate as boundary conditions on the upper part of the cable trays. It is underlined that the mass flowrate is no more predicted as it was done for CFSS-2 in Section 3. The fuel flowrate used as inlet data for the CALIF3S/ISIS calculation is the MLR from experimental measurements in confined conditions as explained in Section 4.3.4.2. The fire boundary condition

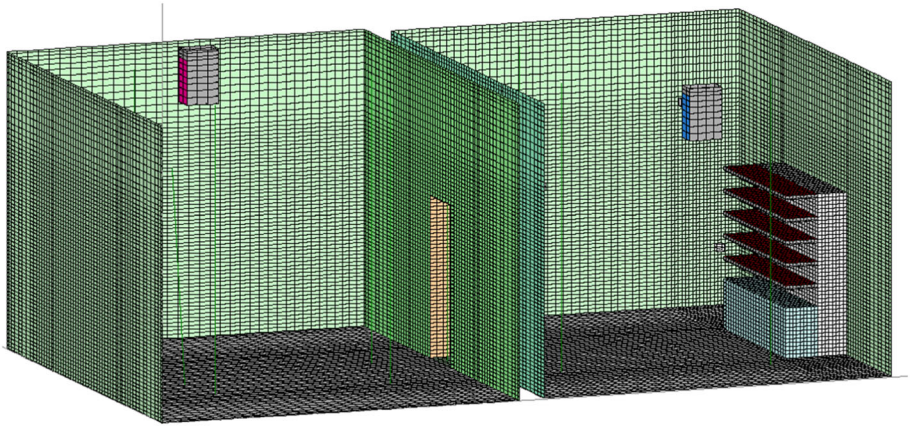

FIGURE 10 View of the DIVA facility modeling with the CALIF3S/ISIS CFD software [Colour figure can be viewed at wileyonlinelibrary.com]

is uniformly applied on the top faces of every cable tray (see Section 4.3.4.2 for more details). The other faces of cable trays are considered as adiabatic.

4.3.2 | Material properties

The conductive heat fluxes are calculated inside the concrete walls and the Thermipan insulation by a Fourier-type modeling. The material properties are detailed hereafter:

- Concrete:
  - conductivity: 1.5 W/m/K
  - specific heat: 736.0 J/kg/K
  - density: 2430.0 kg/m^3
  - emissivity: 0.9
- Thermipan:
  - conductivity: 0.102 W/m/K
  - specific heat: 840.0 J/kg/K
  - density: 140.0 kg/m^3
  - emissivity: 0.95

1.1.1. Meshing and time step

The mesh of fire and adjacent rooms varies in size depending whether they are close to the outer walls or to the floor or close to the fire source (see Figure 10). The total number of cells used for the fluid domain is about 350 000. The mesh size range is presented in Table 5.

From previous studies with CALIF3S/ISIS software,[26,27] this mesh size is considered as appropriate to simulate such fire scenarios.

The time step used for the calculation of CFS-3 is 0.05 second over the 6000 seconds of the scenario. For CFS-4, the time step is 0.05 second, and the simulation duration is 5000 seconds.

4.3.3 | Fire modeling

This section presents the CALIF3S/ISIS modeling of the chemical reaction of the HFFR cables used for the CFS-3 and CFS-4 tests and the modeling of the fire growth rate used in the simulation.

TABLE 5 Mesh sizes for CFS-3 and CFS-4

	Fire Room	Doorway	Adjacent Room
x-axis	5 cm to 10 cm	10 cm	10 cm to 15 cm
y-axis	10 cm to 15 cm	10 cm	10 cm to 15 cm
z-axis	5 cm to 10 cm	5 cm to 7.5 cm	5 cm to 10 cm

Combustion modeling

The combustion modeling is the same as previously presented for the simulation of CFSS-2 (Section 3.2.3.1) since it concerns the same cable type. However, the combustion reaction is fitted in order to take into account the effect of oxygen depletion during each fire test, in particular concerning the carbon monoxide, the soot yields, and the effective heat of combustion.

The combustion reaction is reminded below:

$$C_{3,6}H_{9,6}O_3 + (4.5\text{–}0.5\,co - s)\,O_2 \rightarrow (3.6\text{–}co - s)\,CO_2 + 4.8\,H_2O + co\,CO + s\,C$$

where co and s represent the stoichiometric coefficients of carbon monoxide CO and soot C, defined as follows in the CALIF3S/ISIS modeling:

$$co = \frac{M_{C_{3,6}H_{9,6}O_3} \times y_{co}}{M_{CO}}$$
$$s = \frac{M_{C_{3,6}H_{9,6}O_3} \times y_{soot}}{M_C}$$

where:

- $M_{C_{3,6}H_{9,6}O_3} = 100.8\,g/mol$, is the molar mass of the equivalent combustible fuel $C_{3,6}H_{9,6}O_3$,
- M_C = 12.0 g/mol, is the molar mass of carbon C,
- M_{CO} = 28.0 g/mol, is the molar mass of carbon monoxide CO,
- y_{soot}, is the soot yield given by the experiment,
- y_{co}, is the carbon monoxide yield given by the experiment.

The soot yield measured during the experiment[1] is 0.008 (g/g) for CFS-3 and 0.007 (g/g) for CFS-4. The carbon monoxide yield measured during the experiment is 0.08 (g/g) for CFS-3 and 0.04 (g/g) for CFS-4.

The energy releases during the fire tests are determined by the mean experimental values such as

$$EHC_{CFS-3} = 19.0\ MJ/kg \text{ and } EHC_{CFS-4} = 26.5\ MJ/kg.$$

Fire development

Thanks to the weighting system located beneath the cable tray stack, the mass of pyrolyzed cables can be measured during the experiment. So, the MLR can be determined by calculating the time derivative of the mass evolution during the fire test.

HRRs during the fire tests are determined by both thermal and chemical methods. It is emphasized that the HRR cannot be directly correlated to the MLR in particular in confined and ventilated conditions and oxygen-controlled fires. Indeed, the MLR is representative of the pyrolysis gas production by the cable degradation, while the HRR is representative of the fire power due to the combustion of pyrolysis gas inside the fire room. The main difference lies in combustion efficiency and possibly delayed combustion. Furthermore, the occurrence of successive combustions of unburnt hydrocarbons under the ceiling has been highlighted during the CFS-3 test,[1] involving sharp evolutions of gas temperature, oxygen and carbon dioxide concentrations in the upper part of the fire compartment as well as pressure peaks. For this reason, such an evolution in the experimental HRR has to be taken into account when performing simulations.

Simulations with the CALIF3S/ISIS software are considered by fixing the fuel flowrate as input data. When simulating the CFS tests characterized by a solid fire source, the mass rate of fuel available to be burnt at every time is the mass rate of pyrolysis gas produced from the experiment. However, as mentioned previously, this approach does not allow predicting properly delayed combustions observed during the fire test. Therefore, an "equivalent" mass rate is calculated based on the experimental HRR as a function of time and the average EHC evaluated in the experiment.[1] This attempt aims at simulating more closely the pyrolysis gas consumption by opposition to the pyrolysis gas production. Then, it follows:

$$MLR\_calcul(t) = \frac{HRR\_exp\ (t)}{EHC}$$

where:

- EHC_{CFS-3} = 19.0 MJ/kg and EHC_{CFS-4} = 26.5 MJ/kg are the average EHC[1] determined for CFS-3 and CFS-4, respectively,
- MLR_calcul is the calculated mass rate of consumed pyrolysis gas (kg/s),
- HRR_exp is the experimental HRR obtained during tests (MW).

The experimental MLR and HRR are plotted in Figures 11 and 12 as well as the calculated "equivalent" MLRs of the combustible fuel. It appears that the experimental and calculated MLRs show two different evolutions. First, the calculated MLR reveals large and sharp oscillations corresponding to the fast combustions under the ceiling, while the experimental MLR shows smaller oscillations due to a feedback effect of the radiation from the upper burning layer under the ceiling

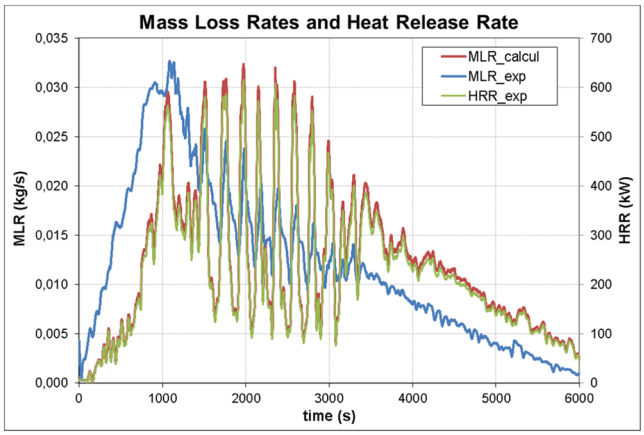

FIGURE 11 Mass loss rate and heat release rate for CFS-3 test [Colour figure can be viewed at wileyonlinelibrary.com]

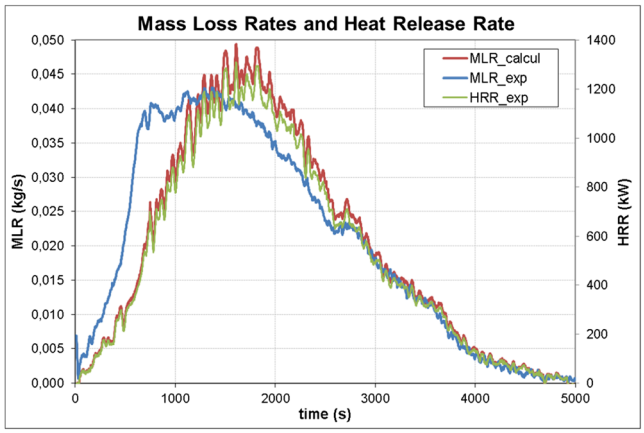

FIGURE 12 Mass loss rate and heat release rate for CFS-4 test [Colour figure can be viewed at wileyonlinelibrary.com]

toward the cable tray fire source for the CFS-3 fire test. The second difference appears at the beginning of the transients where a delay can be observed between the experimental and the calculated MLR rises due to the water mass lost by the fire retardant, which is associated with no fire power release.

Modeling fire propagation along cable trays (ie, the FLASH-CAT approach) is not considered in such a modeling due to the complexity of this fire test (for instance, the effect of oxygen depletion surrounding the cable trays). In this case, the fuel flowrate is uniformly applied on the fire boundary condition for the entire duration of the fire tests. Consequently, it should be emphasized that some local phenomena that may occur within the fire source in the experiment (eg, oxygen depletion effect and locally predominant combustions) cannot be taken into account. Due to the prescribed mass flowrate obtained from the experimental HRR, the fuel release including the combustions observed under the ceiling is then averaged on the tray surface. The propane burner is not modeled in this study.

4.3.4 | Turbulence and radiative heat transfer modeling

The same models as for the CFSS-2 test are used (see Sections 3.2.4 and 3.2.5).

4.4 | Simulation results and discussion

This section aims at presenting the simulation results of the CFS-3 and CFS-4 fire tests with the CALIF3S/ISIS software. Numerical results are compared with the experimental results and concern gas temperatures in the fire room, gas species concentrations, gas pressure, and flowrates at the inlet and outlet openings of the aeraulic circuit.

Unless otherwise stated in this document, the legend of graphs presents the simulation results and the experimental results as follows "isis_x" and "exp_x," respectively, where "x" represents the sensor elevation from the floor of the compartment.

4.4.1 | Simulation results for the CFS-3 fire test

The results presented below concern the simulation of the CFS-3 test characterized by a VRR of 4 per hour.

Pressure and ventilation flowrates

Figures 13 and 14 show the relative pressure of the fire and adjacent rooms, and the mass flowrates at the inlet and outlet openings of the aeraulic circuit, respectively.

The time evolution of the experimental relative pressure in rooms (see Figure 13) shows several peaks (highest value at about 18 hPa), corresponding to the successive combustions of unburnt hydrocarbons accumulated under the ceiling. They lead to flow reversals in the inlet duct and to mass flowrate peaks at the outlet as observed in Figure 14 between about t = 1000 seconds and t = 3500 seconds.

The simulation result for the relative pressure is satisfying compared with the experimental data. The pressure peaks and pressure minima due to the successive combustions are sometimes underestimated by the simulation. However, the oscillatory behavior of the relative pressure in the fire room is well predicted by the CALIF3S/ISIS software.

Concerning the mass flowrates at the inlet and outlet of the aeraulic circuit, the simulation with the CALIF3S/ISIS software also gives good results. Flow reversals at the inlet are predicted when combustions occur under the ceiling and their magnitudes are satisfying.

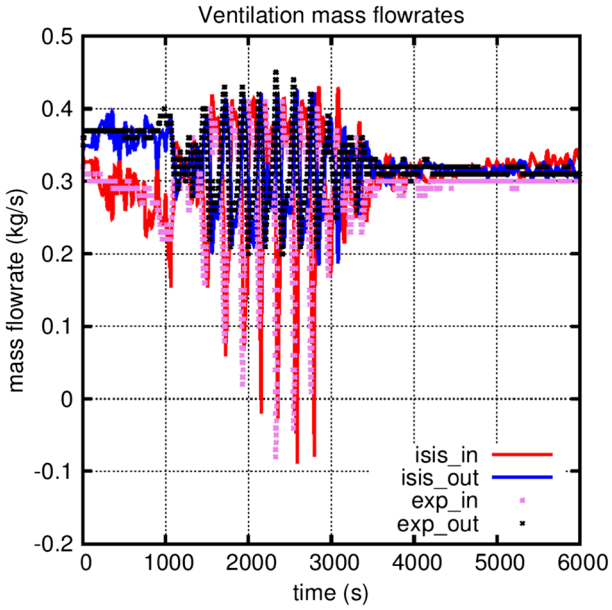

FIGURE 14 Mass flowrates at the inlet and outlet openings of the aeraulic circuit for the CFS-3 test [Colour figure can be viewed at wileyonlinelibrary.com]

Gas temperatures

The following figures (Figures 15, 16, and 17) show comparisons of numerical and experimental gas temperatures at the corners of the fire room.

The experimental temperature evolutions measured at the three corners of the fire room can be divided into three main stages. The first stage of the fire ranging from fire ignition to about 1400 seconds is characterized by the fire growth period, in which temperatures measured on the thermocouple (TC) trees sharply increase during the first

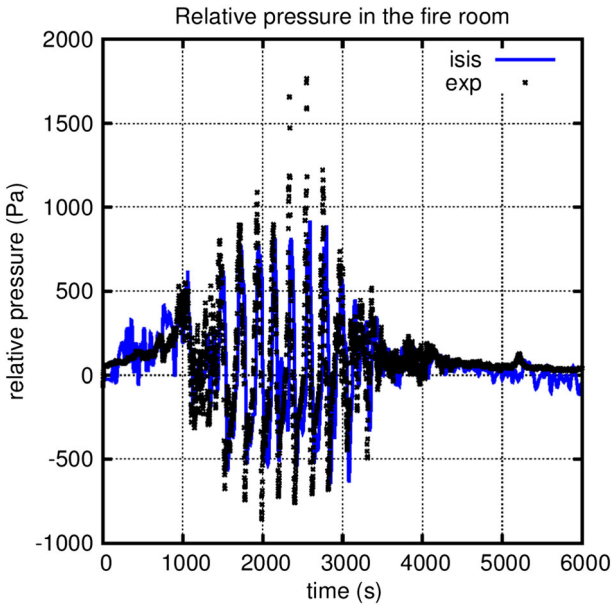

FIGURE 13 Relative pressure in the facility for the CFS-3 test [Colour figure can be viewed at wileyonlinelibrary.com]

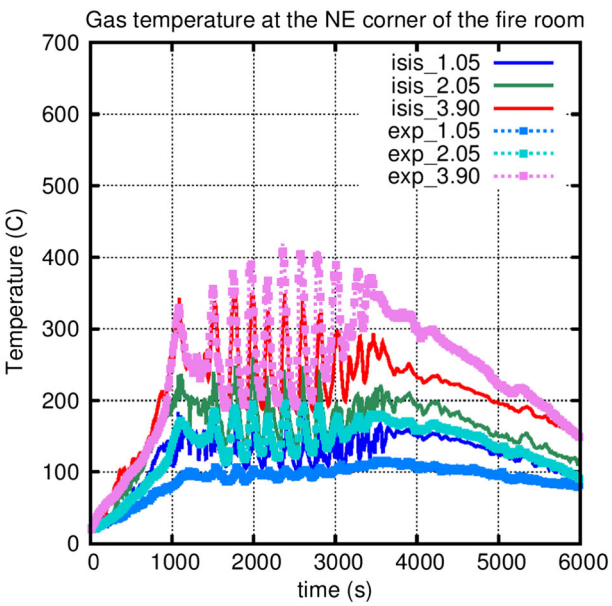

FIGURE 15 Gas temperatures at the NE corner of the fire room for the CFS-3 test [Colour figure can be viewed at wileyonlinelibrary.com]

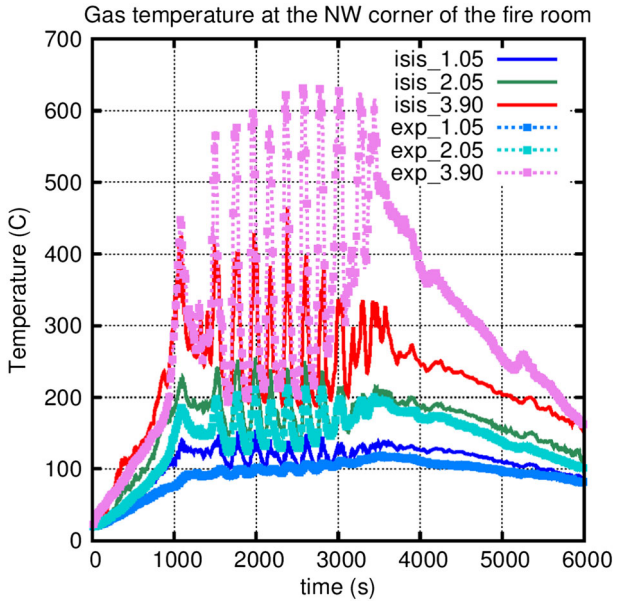

FIGURE 16 Gas temperatures at the NW corner of the fire room for the CFS-3 test [Colour figure can be viewed at wileyonlinelibrary.com]

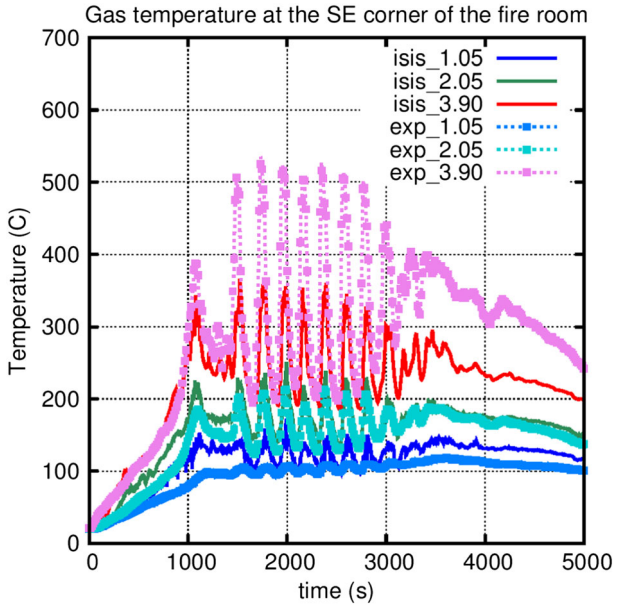

FIGURE 17 Gas temperatures at the SE corner of the fire room for the CFS-3 test [Colour figure can be viewed at wileyonlinelibrary.com]

1070 seconds where a first HRR peak is reached (see Figure 11). Afterwards, during the second stage, from t = 1400 seconds to t = 3500 seconds, the gas temperatures show many oscillations due to fast combustions of unburnt hydrocarbons in the upper part of the fire room. The influence of those fast combustions is therefore more visible on high elevation TCs and in particular at the NW corner whose TCs record the highest temperatures (Figure 16). As a general trend, the mean temperatures are rather steady during this second stage. The third stage is the decay phase of the fire thus leading to temperature decrease.

One particular behavior during this fire scenario concerns the NE corner of the fire room where the experimental temperature at elevation z = 3.90 m is the lowest (Figure 15). Indeed, the maximum temperature is about 420°C, while it is about 530°C at the SE corner and 640°C at the NW corner (Figures 17 and 16). This location is right in the vicinity of the air inlet opening which occupies the last 60 cm below the ceiling (between elevations z = 3.60 m and z = 4.00 m). The influence of the air opening seems to be limited to the very upper part of the corner close to the ceiling and in front of the opening, as the VRR is low in the CFS-3 test.

Concerning the gas temperature in the fire room, the numerical results are overall mostly overestimated in the lower part, quite well predicted at the mid-plane and then mostly underestimated at 3.9 m. This is certainly due to the fact that the experimental temperatures at the top are particularly high as fast combustions of unburnt hydrocarbons take place under the ceiling. Conversely, in the modeling, the corresponding amount of energy is released all over the cable tray top faces located far beneath the ceiling. This would therefore explain the underestimation at the top and the overestimation at the bottom of the fire room. It is underlined that the CALIF3S/ISIS modeling does not allow modeling these local phenomena.

Gas concentrations

The oxygen and carbon dioxide concentrations in the fire room at three elevations are presented hereafter.

The oxygen concentration measured in the fire room (Figure 18) decreases with the fire growth and full development up to about t = 1070 seconds in the upper part of the room. Afterwards, as for gas temperatures, the oxygen concentration shows several oscillations. The oxygen concentration is particularly low at z = 3.2 m when fast combustion occurs, thus leading to oxygen concentration downs to about 2.5%. Conversely, at elevation z = 0.7 m, the oxygen concentration reaches a plateau at about 13%. In between, at elevation z = 2.2 m, oscillations are also visible during the second stage of the fire, but the average oxygen concentration is quite close to the one at z = 0.7 m. Consequently, a strong oxygen concentration gradient

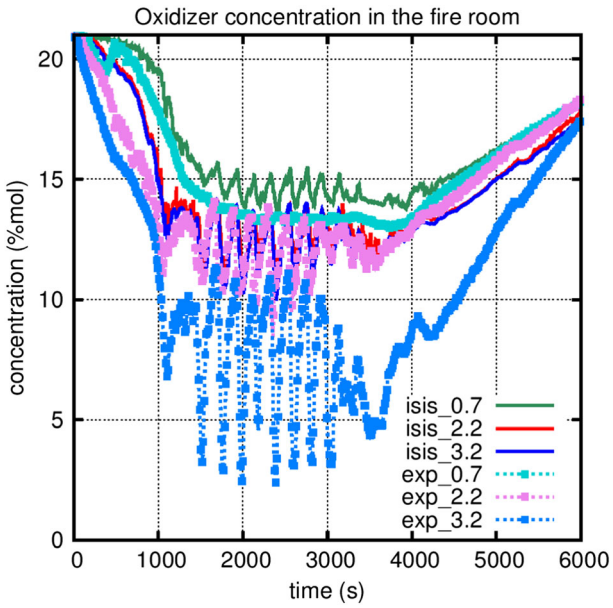

FIGURE 18 Oxygen concentrations in the fire room for the CFS-3 test [Colour figure can be viewed at wileyonlinelibrary.com]

is noticed in the very upper part of the fire room. This is to be linked with the fast combustions taking place under the ceiling and therefore reducing the already low oxygen content nearby. The carbon dioxide concentrations evolve accordingly (Figure 19).

Concerning the simulated results in the fire room, the CALIF3S/ISIS software predicts an oxygen concentration fall a little too gentle compared with the experiment (Figure 18), in particular for elevations z = 3.2 m and z = 2.2 m. However, the predicted results are quite satisfying at elevations z = 0.7 m and z = 2.2 m for the whole transient duration. The major discrepancy concerns elevation z = 3.2 m where the oxygen concentration fall is also predicted far too short, as a result, the simulated oxygen concentration is far overestimated. For example, during the second phase of the fire transient, the average oxygen concentration predicted by the CALIF3S/ISIS software is about 12%, while in the experiment it is about 7% (with large oscillations from 2% to 12%). It is emphasized that in the simulation, concentrations at z = 2.2 m and z = 3.2 m are similar, which is by far not the case in the experiment. This tends to illustrate that the local phenomena occurring under the ceiling are not taken into account by the modeling. Concerning carbon dioxide concentrations in the fire room, the numerical results are consistent with those of the oxygen concentrations. They are in good accordance with the experiment at elevations z = 0.7 m and z = 2.2 m, but the carbon dioxide concentration is underestimated at elevation z = 3.2 m (Figure 19). For the latter elevation, the oscillation magnitude is far underestimated by the CALIF3S/ISIS software. As already mentioned in Section 3.2.3.1, some discrepancies regarding oxygen consumption and carbon dioxide production might be due to not taking into account the accurate PE input through the proportion of PE compared with EVA in the PE/EVA copolymer. For example, considering the available data in Figure 18, the oxygen concentration overestimation in the upper part of the fire room is not compensated for by an underestimation elsewhere in the room.

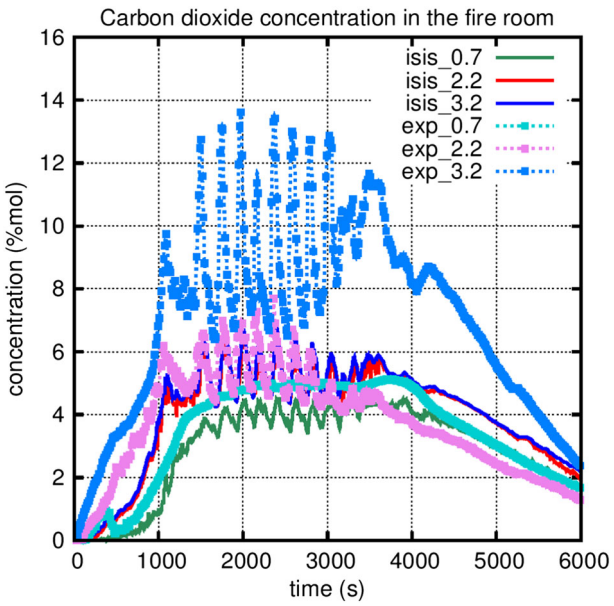

FIGURE 19 Carbon dioxide concentrations in the fire room for the CFS-3 test [Colour figure can be viewed at wileyonlinelibrary.com]

4.4.2 | Simulation results for the CFS-4 fire test

The results presented below concern the simulation of the CFS-4 fire test characterized by a high VRR of 15 per hour.

Pressure and ventilation flowrates

Figures 20 and 21 show the relative pressure of the fire and adjacent rooms, and the mass flowrates at the inlet and outlet openings of the aeraulic circuit, respectively.

The time evolution of experimental relative pressure in rooms (see Figure 20) shows a period of somewhat scattered points between

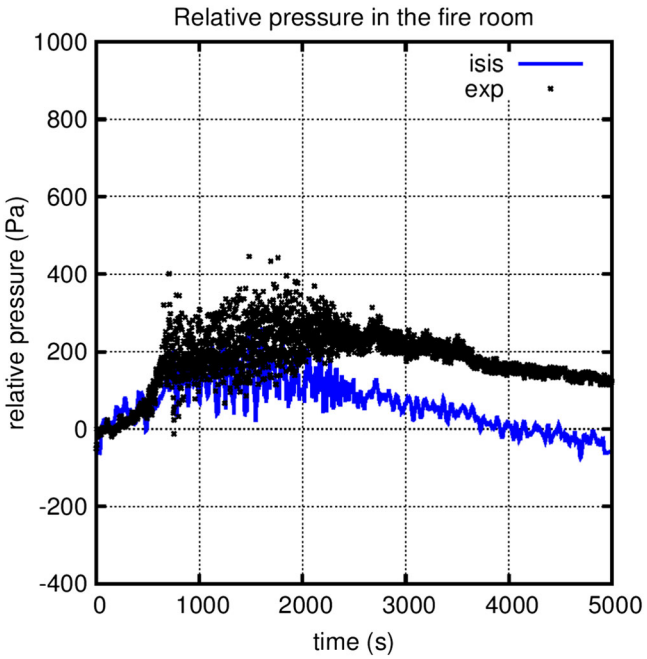

FIGURE 20 Relative pressure in the facilityfor the CFS-4 test [Colour figure can be viewed at wileyonlinelibrary.com]

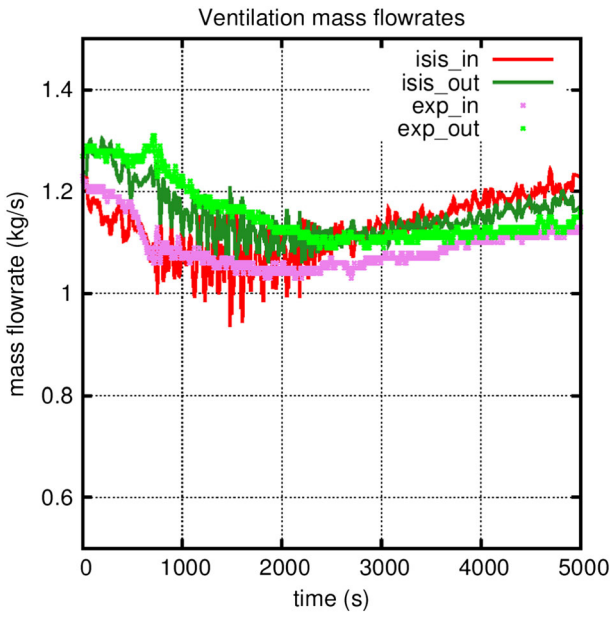

FIGURE 21 Mass flowrates at the inlet and outlet openings of the aeraulic circuit for the CFS-4 test [Colour figure can be viewed at wileyonlinelibrary.com]

about t = 800 seconds and t = 2500 seconds with relative pressure oscillations at high frequency and with a magnitude about 2 to 3 hPa. The origin of these variations is not determined yet. About the pressure evolution, the aeraulic resistance during the CFS-4 test was quite reduced thus limiting any pressure peak. As a consequence, flow reversals are not observed at the inlet duct of the ventilation circuit (Figure 21), and the flowrates at the openings have quite smooth evolutions.

The simulation result for the relative pressure evolution is satisfying compared with the experiment, in particular during the first 2000 seconds of the fire. Afterwards, the relative pressure is slightly underestimated by the CALIF3S/ISIS software. At the end of the fire, the software predicts pressure similar to the one at the beginning of the calculation while the experimental value at the end is greater than its initial value. The wall heat fluxes after the particularly powerful CFS-4 fire may account for a greater pressure at the end of the fire in the experiment.

Concerning the mass flowrates at the inlet and outlet of the aeraulic circuit, the simulation with the CALIF3S/ISIS software gives good results. The outlet mass flowrate is slightly underestimated during the first part of the fire, but the relative discrepancy is limited to about 5%. Both mass flowrates are slightly overestimated (below 10%) at the end of the transient. However, in the same way as indicated for the pressure evolution, the mass flowrates in the experiment have a lower value at the end than at the beginning of the fire.

Gas temperatures

The following figures (Figures 22, 23, and 24) show gas temperature at the corners of the fire room.

The experimental temperature evolutions measured at the three corners of the fire room can be divided into two main stages. The first stage of the fire up to about 1800 seconds is characterized by the fire growth where temperatures measured on the TC trees increase and a HRR peak is reached (see Figure 12) with some small oscillations. The second stage is the decay phase of the fire thus leading to HRR and temperature decrease.

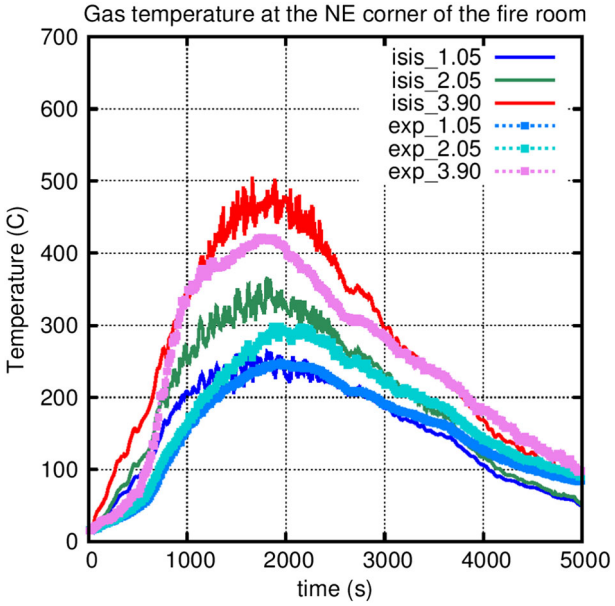

FIGURE 22 Gas temperatures at the NE corner of the fire room for the CFS-4 test [Colour figure can be viewed at wileyonlinelibrary.com]

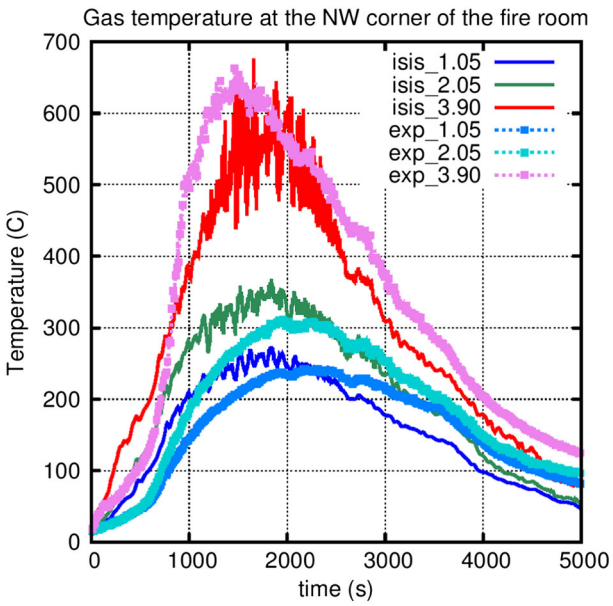

FIGURE 23 Gas temperatures at the NW corner of the fire room for the CFS-4 test [Colour figure can be viewed at wileyonlinelibrary.com]

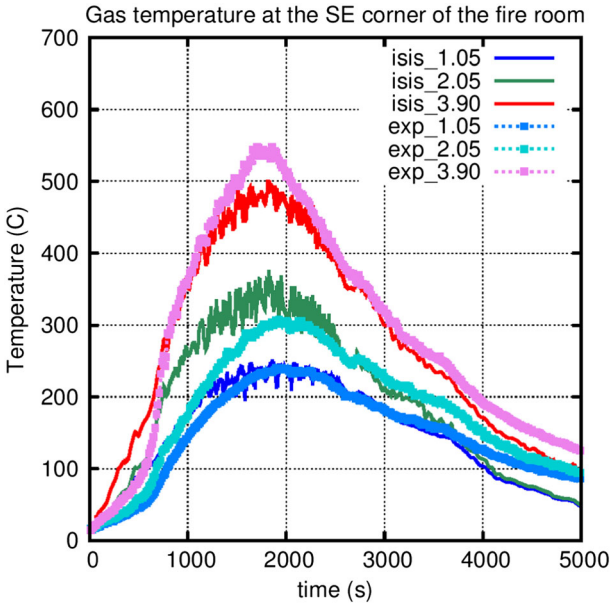

FIGURE 24 Gas temperatures at the SE corner of the fire room for the CFS-4 test [Colour figure can be viewed at wileyonlinelibrary.com]

One particular behavior concerns the NE corner of the fire room where the lowest experimental temperature at elevation z = 3.90 m is recorded (Figure 22). This location is right in the vicinity of the air inlet opening. This comment is the same as for CFS-3 in Section 4.4.1.2.

Concerning gas temperatures in the fire room, the numerical results are overall in good agreement with the experimental results in both the upper and lower part of the room. The discrepancy is generally limited to 20% with one exception. This one is for elevation z = 3.9 m at the NW corner (Figure 23) where the predicted temperature shows a large number of oscillations with a high magnitude up

to 150°C. The maximum values predicted for the NW temperature are in quite good agreement with the experiment, which is not the case of the lowest oscillation values.

Gas concentrations

The oxygen and carbon dioxide concentrations in the fire room at three elevations are presented hereafter (Figures 25 and 26).

In Figure 25, the oxygen concentration measured in the fire room decreases with the fire growth and full development up to about t = 1800 seconds at elevation z = 2.2 m and z = 0.7 m and then rise until the end of the transient. At elevation z = 3.2 m, the oxygen concentration rapidly falls down to a value of about 5% and then suddenly rises at about t = 1600 seconds. This is due to the 3.2-m-high sensor

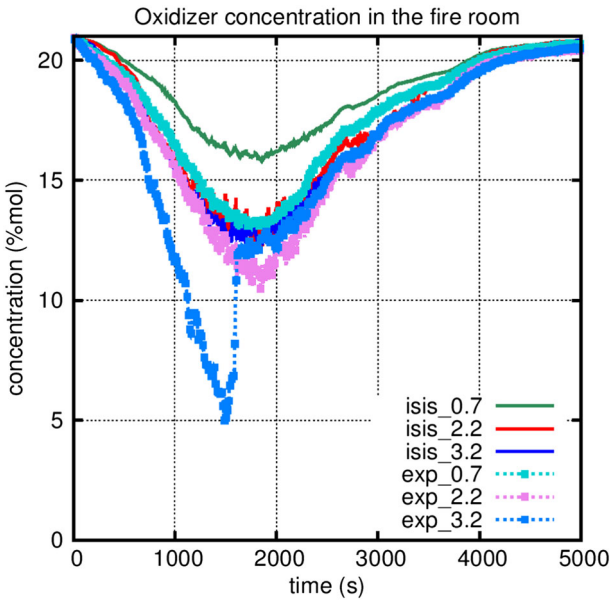

FIGURE 25 Oxygen concentrations in the fire room for the CFS-4 test [Colour figure can be viewed at wileyonlinelibrary.com]

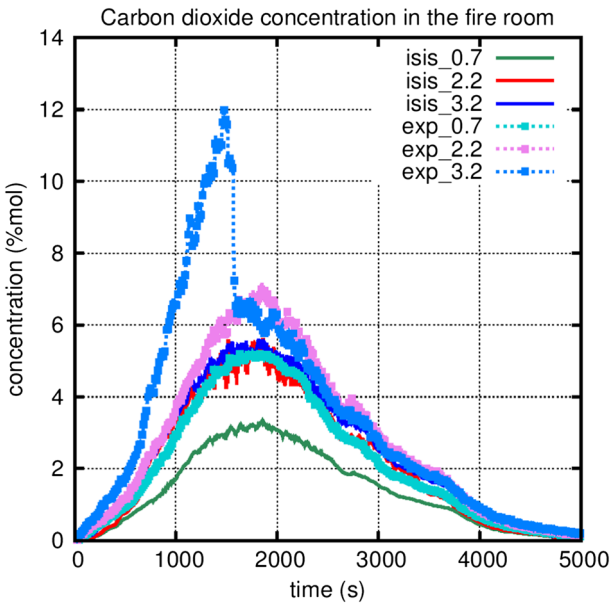

FIGURE 26 Carbon dioxide concentrations in the fire room for the CFS-4 test [Colour figure can be viewed at wileyonlinelibrary.com]

falls from its support. Therefore, after this fall, its measure is no more reliable as for the carbon dioxide measurement. For the two other elevations, the carbon dioxide concentrations evolve in accordance with the oxygen concentrations.

The numerical results in the fire room underestimate the oxygen concentration decrease at elevation z = 0.7 m and in particular at z = 3.2 m. For the latter elevation, when the minimum of 5% is reached, the simulated concentration is only about 13%, and its minimum value on the whole duration of the test is only about 12%. In fact, the oxygen concentration at z = 3.2 m is predicted quite similar to the one at z = 2.2 m thus underestimating the axial oxygen concentration gradient. However, the oxygen concentration at z = 2.2 m is well predicted by the CALIF3S/ISIS software. Concerning carbon dioxide concentrations in the fire room, the same comments can apply, ie, the carbon dioxide concentration is underestimated at z = 0.7 m (maximum 30% discrepancy), far underestimated at z = 3.2 m and then quite well predicted at the mid-plane. No axial carbon dioxide concentration is predicted between z = 2.2 m and z = 3.2 m, which is, by far, not the case in the experiment. As for the CFS-3 test in Section 4.4.1.3, a comment may be done concerning taking into account a greater content of PE in the cable composition. This may increase the oxygen consumption and the carbon dioxide production (see Section 3.2.3.1).

5 | CONCLUSION AND PROSPECTS

This section presents the simulation of the CFSS-2, CFS-3, and CFS-4 fire tests with the CALIF3S/ISIS software. The CFSS-2 test is a cable tray stack fire test carried out under a large-scale calorimeter in open atmosphere. The cables are control-type and are composed of a polymer sheath containing HFFR (alumina tri-hydrate). The CFS-3 and CFS-4 tests are performed in confined and mechanically ventilated conditions with the same fire source as in the CFSS-2 tests.

For the simulation of the CFSS-2 fire test, the fire source is modeled in accordance with the experiment, ie, the five horizontal cable trays are individually modeled using the dimensions of the experimental setup. Fire propagation along trays and from one tray to another is predicted by means of a FLASH-CAT-like model implemented on purpose in the CALIF3S/ISIS software. This empirical model is based on a timing sequence for the upward propagation only depending on the tray order in the stack. It also suggests that the cables should burn over a length that is greater than that of the tray below, thus leading to a V-shaped fire pattern expanding with the horizontal propagation. The parameters of this model are optimized thanks to a video analysis of the fire experiment. The advantage of this simple approach is to assess properly the burning surface at every moment.

The simulation with the CALIF3S/ISIS software of the CFSS-2 test is performed, and the predicted MLR and HRR are compared with the experimental data. In both cases, the fire growth rate, from fire ignition up to the HRR peak, is well predicted by CALIF3S/ISIS despite a predicted MLR evolution a little later than in the experiment. This is caused by the preliminary mass loss due to the decomposition of the fire retardant that releases water vapor. This mass loss cannot be taken into account by the model when it is associated with no heat release at the beginning of the fire. The MLR and HRR peaks are well

predicted. Afterwards, the fire decay is predicted a little too slow for a short period. Then, the fire decay is predicted sharper than the experiment and fire extinction is predicted too early. On a safety point of view, this result is conservative since it tends to overestimate the duration at high fire power. Moreover, the TML and the total heat release are well predicted. Consequently, the simulation of the CFSS-2 test with the CALIF3S/ISIS software gives satisfying results.

The simulation of CFS-3 and CFS-4 tests with CALIF3S/ISIS is performed using the same fire source modeling as for CFSS-2. However, for these confined and ventilated tests, fire propagation is no more computed. Instead, the fire boundary condition is uniformly applied on the top faces of trays and uses a MLR determined from experimental data, ie, the HRR and the effective heat of combustion. This method enables to take into account delayed combustions and to avoid considering the MLR induced by the decomposition of the fire retardant at the beginning of the fire tests.

The comparison between the numerical results and the experimental data shows overestimated gas temperatures in the fire room in the lower part and underestimated in the upper part for the simulation of the CFS-3 test. In the experiment, many fast combustions occurred under the ceiling and calculation failed to properly locate the corresponding power release. For the CFS-4 test, temperatures are overall well predicted in a range of a 20% discrepancy from the experiment. Concerning oxygen and carbon dioxide concentrations in the fire room in both confined fire tests, overall oxygen consumption and carbon dioxide production underestimations are observed. It may be due to inaccurate mass composition and representativeness of the considered fuel, in particular due to the lack of considering the accurate proportion between PE and EVA in the PE/EVA copolymer. To end with, the relative room pressure and the mass flowrates at the inlet and outlet openings of the ventilation circuit are satisfying compared with the experiment for both the CFS-3 and CFS-4 tests.

Modeling the five trays along with the MLR applied on its surfaces does not allow to model some local phenomena since the burning surface is considered uniform on the whole fire boundary condition for the entire test duration. Consequently, no distinction is made between trays and the total heat release is relocated to the fire source place, even in the case of a heat release due to a fast combustion of unburnt hydrocarbons under the ceiling. However, the CALIF3S/ISIS simulation results are quite satisfying as the overall behavior of the fire transients is well reproduced, especially considering the fire transient complexities.

In order to go further in simulating electric cable fires in confined conditions and in order to perform more predictive simulations, fire propagation along trays and from one tray to another should be calculated. The fire propagation prediction with the CALIF3S/ISIS software and the FLASH-CAT-like model with optimized parameters depending on the fire configuration give good results in open conditions as shown with the simulation of the CFSS-2 fire. A more detailed and more predictive approach would consist in calculating the fire spread rate instead of using velocities obtained from experimental observations. This task is in progress as IRSN is planning to develop and implement analytical relations making the link between the ignition times and horizontal propagation rates and the physical parameters of cables (material properties) and cable tray configurations (cable load, tray width...). Predicting fire propagation for fire tests in confined and ventilated condition is much more complex and needs to take into account the oxygen limitation close to the cable fire. Even though oxygen limitation is quite well known for liquid pool fires, it is not the case for complex solid fuels such as electric cables. IRSN is addressing these subjects through ongoing research and development programs featuring experimental and computational efforts to model electric cable fires.

ACKNOWLEDGEMENT

The authors of this document are grateful for the financial support of the members participating to the joint OECD PRISME-2 program: ENGIE and Bel V (Belgium), CNSC (Canada), VTT (Finland), DGA and EDF (France), GRS (Germany), NRA and CRIEPI (Japan), CSN (Spain), SSM (Sweden), and ONR, an agency of HSE (United Kingdom).

ORCID

Sophie Bascou http://orcid.org/0000-0002-7645-0281
Pascal Zavaleta http://orcid.org/0000-0001-7998-0627

REFERENCES

1. Zavaleta P, Audouin L. Cable tray fire tests in a confined and mechanically ventilated facility. *Fire Mater*. 2017;42(1):1-16. https://doi.org/10.1002/fam.2454
2. Sumitra PS. Categorization of cable flammability, intermediate-scale fire tests of cable tray installations, interim report NP-1881, Research Project 1165–1161, Factory Mutual research Corp, Norwood, MA, USA. 1982.
3. Grayson SJ, Van Hees P, Green AM, Breulet H, Vercellotti U. Assessing the fire performance of electric cables (FIPEC). *Fire Mater*. 2001;25(2):49-60.
4. McGrattan K, Lock A, Marsh N, et al. Cable heat release, ignition and spread in tray installations during fire (CHRISTIFIRE) phase 1: horizontal trays, NUREG/CR-7010. 2012;1.
5. McGrattan K, Bereham S. Cable heat release, ignition, and spread in tray installations during fire (CHRISTIFIRE) phase 2: vertical shafts and corridors, NUREG/CR-7010. 2013;2.
6. Audouin L, Pretrel H, Zavaletta P. 2013, OECD PRISME 2 Fire Research Project (2011–2016)—current status and perspectives, SMiRT 22 13th International Seminar on Fire Safety in Nuclear Power Plants and Installations, Columbia, SC, USA.
7. Zavaleta P, Audouin L. Fire spreading from a real open-doors electrical cabinet to overhead multiple cable trays into a confined and mechanically-ventilated facility, Conference proceedings of the fourteenth international INTERFLAM conference, University of London, UK. 2016:1563-1574.
8. Zavaleta P, Charbaut S, Basso G, Audouin L. Multiple horizontal cable tray fire in open atmosphere. In: Thirteenth international conference of the fire and materials, San Francisco 2013:57-68.
9. SYLVIA (n.d.), Collaborative website: https://gforge.irsn.fr/gf/project/sylvia/
10. CALIF3S/ISIS software (n.d.-a), Collaborative website: https://gforge.irsn.fr/gf/project/isis/
11. Dey MK. Evaluation of fire models for nuclear power plant applications: cable tray fires, NIST Internal Panel Report NISTIR 6872, 2002.
12. Röwekamp M, Klein-Hessling W, Riese O, Berg PH. Flame spread in cable tray fires and its modeling in fire simulation codes. *J KONBiN*. 2008;3(6):2008. ISSN 1895-8281.
13. Beji T, Verstockt S, Zavaleta P, Merci B. Flame spread monitoring and estimation of the heat release rate from a cable tray fire using video fire analysis (VFA). *Fire Technol*. 2016;52(3):611-621.

14. CALIF3S/ISIS software (version 4.0.0), Physical modeling report, 2014a https://gforge.irsn.fr/gf/project/isis/docman/Physical%20modelling/
15. Cox G. *Combustion Fundamentals of Fire*. Academic Press; 1995.
16. Chai JC, Lee HS, Patankar SV. Finite volume method for radiation heat transfer. *J Thermophys Heat Transfer*. 1994;8(3):419-425.
17. Raithby GD, Chui EH. A finite-volume method for predicting a radiant heattransfer in enclosures with participating media. *J Heat Transfer (Trans ASME)* 1990;112(2):415–423.
18. Smith TF, Shen ZF, Friedman JN. Evaluation of coefficients for the weighted sum of gray gases model. *J Heat Transfer (Trans ASME)*. 1982;104(4):602-608.
19. Babik F, Gallouët T, Latché J-C, Suard S, Vola D. On two fractional step finite volume and finite element schemes for reactive low Mach number flows. In: *The International Symposium on Finite Volumes for Complex Applications IV—Problems and Perspectives*. Marrakech; 2005.
20. CALIF3S/ISIS software (version 4.0.0), Validation report, 2014b https://gforge.irsn.fr/gf/project/isis/docman/Validation/
21. Meinier R, Sonnier R, Zavaleta P, Suard S, Ferry L. Fire behavior of halogen-free flame retardant electrical cables with the cone calorimeter. *J Hazard Mater*. 2017;342:306-316. https://doi.org/10.1016/j.jhazmat.2017.08.027
22. Brossas J. Retardateurs de flammes, techniques de l'ingénieur, AM3237. 1999.
23. Morgan AB, Gilman JW. An overview of flame retardancy of polymeric materials: application, technology, and future directions, *J Fire Mater*, 2013;37:259–279.
24. U.S. NRC and EPRI. Fire PRA methodology for nuclear power facilities, NUREG/CR-6850, U.S. Nuclear Regulatory Commission, Washington, DC. 2004.
25. Drysdale D. *An Introduction to Fire Dynamics*. Third ed. Edinburgh: John Wiley & Sons; 2011.
26. Perez Segovia JF, Beji T, Merci B. CFD simulations of pool fires in a confined and ventilated enclosure using the Peatross-Beyler correlation to calculate the mass loss rate. *Fire Technol*. 2017;53(4):1669-1703.
27. Pretrel H, Suard S, Audouin L. Experimental and numerical study of low frequency oscillatory behavior of a large-scale hydrocarbon pool fire in a mechanically ventilated compartment. *Fire Saf J*. 2016;83(2016):38-53.

How to cite this article: Bascou S, Zavaleta P, Babik F. Cable tray FIRE tests simulations in open atmosphere and in confined and mechanically ventilated compartments with the CALIF3S/ISIS CFD software. *Fire and Materials*. 2019;43:448–465. https://doi.org/10.1002/fam.2680